Sequence analysis of the 5′ untranslated region of swine vesicular disease virus reveals block deletions between the end of the internal ribosomal entry site and the initiation codon

Andrew E. Shaw,[1] Scott M. Reid,[1] Nick J. Knowles,[1] Geoffrey H. Hutchings,[1] Ginette Wilsden,[1] Emiliana Brocchi,[2] David Paton[1] and Donald P. King[1]

Correspondence
Donald P. King
donald.king@bbsrc.ac.uk

[1]Institute for Animal Health, Ash Road, Pirbright, Surrey GU24 0NF, UK

[2]Department of Research, Istituto Zooprofilattico Sperimentale della Lombardia e dell'Emilia Romagna, Via Bianchi 7/9, 25124 Brescia, Italy

Received 23 February 2005
Accepted 29 June 2005

Swine vesicular disease virus (SVDV) is a picornavirus closely related to the human pathogen coxsackievirus B5. In common with other picornaviruses, the 5′ untranslated region (5′ UTR) of SVDV contains an internal ribosomal entry site (IRES) that plays an important role in cap-independent translation. The aim of this study was to use RT-PCR and sequencing to characterize a fragment of the 5′ UTR encompassing the entire IRES. Sequence analysis demonstrated high nucleotide identities within the IRES between 33 representative SVDV isolates. These data support the choice of this region as a diagnostic target and provide information for the improvement of laboratory-based molecular assays to detect SVDV. In contrast to the relative conservation of the IRES element, there was considerable nucleotide variability in the spacer region located between the cryptic AUG at the 3′ end of the IRES and the initiation codon of the polyprotein. Interestingly, 11 SVDV isolates had block deletions of between 6 and 125 nt in this region. Nine of these isolates were of recent European origin and were phylogenetically closely related. *In vitro* growth studies showed that selected isolates with these deletions had a significantly reduced plaque diameter and grew to a significantly lower titre relative to an isolate with a full-length 5′ UTR. Further work is required to define the significance of these deletions and to assess whether they impact on the pathogenesis of SVD.

INTRODUCTION

Swine vesicular disease (SVD) is a highly contagious viral disease of domestic pigs. The causative agent, swine vesicular disease virus (SVDV), belongs to the genus *Enterovirus* within the family *Picornaviridae*. It is a non-enveloped virus with a single-stranded positive-sense RNA genome of approximately 7·4 kb. The virus is both antigenically and genetically related to the human pathogen coxsackievirus B5 (CV-B5), although pigs inoculated with CV-B5 do not show overt clinical signs of SVD (Garland & Mann, 1974). SVD was first recognized in Italy in 1966 (Nardelli *et al.*, 1968). Since then, outbreaks have been reported across Europe and in the Far East. Although SVDV was largely eradicated from Europe during the 1970s and 1980s, a new strain of SVDV, possibly originating in the Far East (Brocchi *et al.*, 1997), entered Europe during 1992. This strain subsequently spread to The Netherlands, Belgium, Portugal, Spain and Italy. In 2003/4, clinical outbreaks of SVD were only reported in Portugal, leading to the slaughter of 2168 pigs, while subclinical infection is continuously detected in Southern Italy (following active virological surveillance).

SVD spreads rapidly through contact with infected pigs and following exposure to a contaminated environment (Dekker *et al.*, 1995), and can cause up to 100 % morbidity in affected pens where animals are in direct contact. The disease is variable, but mild or subclinical infections now predominate in Italy, where there has been the greatest number of reported cases of the disease in the last 10 years. Pathogenic strains of SVDV can produce lesions on the snout and feet which are indistinguishable from those produced by the other vesicular disease viruses, namely foot-and-mouth disease (FMD) virus, vesicular stomatitis (VS) virus and vesiviruses [which include vesicular exanthema of swine virus (VESV)]. Due to the similarity of these clinical signs to FMD, SVD is a notifiable disease and therefore swift,

The GenBank/EMBL/DDBJ accession numbers of the sequences determined in this paper are AY875984–AY876011.

accurate and sensitive diagnosis is necessary for effective disease control. Laboratory differentiation of SVDV from other vesicular disease viruses in clinical samples (typically faeces or vesicular epithelium) can be achieved by a combination of virus isolation (VI) in a permanent line of IB-RS-2 cells (De Castro, 1964) and an antigen ELISA (Ferris & Dawson, 1988). Whilst the ELISA is rapid, producing a result within a few hours, it has a limited sensitivity. VI is a sensitive method, but it can take up to 7 days to produce a definitive result, and other enteroviruses present in faeces can interfere with the isolation of SVDV. Recently, molecular methods, such as RT-PCR, have become more widely accepted for pathogen diagnosis (Belak & Thoren, 2001). An RT-PCR preceded by immune-extraction of SVDV from faeces samples (Fallacara *et al.*, 2000) is routinely used in Italy for the virological surveillance programme, leading to the rapid and sensitive detection of pathogens. Real-time PCR may add further advantages, as it eliminates the need for post-PCR processing stages, such as gel electrophoresis. Two real-time RT-PCR assays have recently been developed for the detection of SVDV (Reid *et al.*, 2004a). Both of these assays target separate locations within the internal ribosomal entry site (IRES) located within the 5′ untranslated region (5′ UTR), which for SVDV is approximately 750 nt in length. This region was chosen as a diagnostic target because the IRES is critical for cap-independent translation and its structure is conserved in many other species of picornavirus (Belsham & Jackson, 2000). Indeed, the primers and probes targeting this region have broad sensitivity against phylogenetically diverse SVDV isolates (Reid *et al.*, 2004a). However, nucleotide substitutions in the TaqMan probe regions resulted in the failure of both assays to detect a single (but different) SVDV isolate (Reid *et al.*, 2004a). Since the design of these real-time RT-PCR primers and probes was based upon just four IRES sequences available in GenBank (Seechurn *et al.*, 1990; Inoue *et al.*, 1989, 1993; Rebel *et al.*, 2000), the aim of this project was to generate additional sequence information for this region from a diverse selection of SVDV isolates, thereby facilitating the development of improved diagnostic assays. Interestingly, during the course of these analyses, large deletions located between the 3′ end of the IRES and the initiation codon of the polyprotein were observed for the sequences of some isolates. In an attempt to investigate the significance of these deletions, *in vitro* growth studies were performed using these isolates.

METHODS

SVDV samples. Infected material from 28 isolates representing all of the seven recognized phylogenetic groups of SVDV (Zhang *et al.*, 1999) was selected for this study (Table 1). These samples comprised both archival and recently circulating isolates from Europe and Asia, and included both homogenates of original clinical samples (epithelial suspensions) and cell-free supernatant material derived from passage of the viruses in IB-RS-2 cells.

RT-PCR and sequencing. Viral RNA was extracted from 200 μl of the starting material from each of the SVDV isolates using Trizol reagent (Invitrogen) according to the manufacturer's instructions, resuspended in 20 μl nuclease-free water (Promega) and stored at −80 °C. cDNA was synthesized using random hexamers (Promega), 10 μl of prepared RNA and M-MLV reverse transcriptase (Invitrogen), as previously described (Reid *et al.*, 2004a). PCR primers (Table 2) were designed based on an alignment of available sequences in GenBank (accession nos D00435, D16364, X54521 and AF268065) to amplify a 763 nt fragment of the SVDV 5′ UTR corresponding to nucleotides 12–774 of the UKG 27/72 (X54521) complete genome sequence. This amplified product encompasses the polyprotein initiation codon (at position 743) and both of the primer-probe sets (2B-IR and 3-IR) designed for the real-time RT-PCR assays (Reid *et al.*, 2004a).

PCR reactions were prepared to a final volume of 50 μl and contained 2 mM $MgCl_2$ (Invitrogen), 50 mM KCl, 10 mM Tris/HCl, pH 8·0 (Thermo Buffer, Invitrogen), 0·25 mM of each dNTP, 20 pmol of each primer and 2·5 U *Taq* DNA polymerase (Invitrogen). Amplification (MJ Research, Inc. thermal cycler) was carried out using the following conditions: 94 °C for 60 s, 61 °C for 60 s, 72 °C for 45 s for 35 cycles. Chain elongation at 72 °C was extended to 7 min for the final cycle. PCR products were visualized by electrophoresis using 1·2 % agarose gels stained with ethidium bromide.

Amplicons of the predicted size were excised from the gels, purified using the QIAquick gel-extraction kit (Qiagen) and quantified with the E-gel low range marker (Invitrogen). Approximately 50 ng of the purified PCR product was directly sequenced on both strands by the chain-termination method, employing the primers shown in Table 2, according to the manufacturer's instructions (Beckman Coulter, CEQ 8000 DNA analysis system). The resulting sequence of each isolate was assembled independently using SEQMAN (DNAStar, Lasergene) and aligned with other sequences using CLUSTAL X (Thompson *et al.*, 1994) and MegAlign (DNAStar, Lasergene). GCG (Wisconsin Package version 10.3, Accelrys Inc., San Diego) was used to determine nucleotide identity between isolates, and nucleotide variability was assessed using an algorithm described elsewhere (Proutski & Holmes, 1998). RNA folding was performed using RNAStructure version 3.5 (Mathews *et al.*, 1999) and RNA DRAW version 1.1 (Mazura Multimedia, Sweden).

PCR analysis of 5′ UTR spacer region. Surprisingly, several isolates had deletions in the 5′ UTR spacer region which prompted further investigation. SVDV isolates were screened by RT-PCR to identify those with 5′ UTR spacer deletions. cDNA (2·5 μl) prepared as above was amplified using primers SASVD-3-IR-455-473F and SVD-5UTR REV3 (Table 2). Amplification conditions were as follows: 94 °C for 60 s, 63 °C for 45 s, 72 °C for 45 s for 35 cycles. Chain elongation at 72 °C was extended to 7 min for the final cycle. PCR products were analysed as described above and compared with the band size produced by viruses that had already been sequenced.

Virus plaque diameter. Titrations of the stock virus were performed in initial plaquing experiments to determine the viral titre (plaque forming units ml^{-1}). Petri dishes confluent with IB-RS-2 cells were then inoculated with 0·5 ml of a dilution containing approximately 100 p.f.u. of stock virus. The virus was allowed to adsorb for 30 min and excess virus was removed by needle and syringe. Eight millilitres of overlay [MEM in 1·6 % Noble agar (Difco Laboratories) supplemented with 0·1 % fetal calf serum (Sigma)] was then added and allowed to set. Plates were incubated at 37 °C and plaques visualized at 72 h after methylene-blue staining. The diameters of the resulting plaques were measured.

Time-course study of virus growth. The growth of selected SVDV isolates in confluent IB-RS-2 cells was monitored in 25 cm^3 flasks (Falcon). After washing off the maintenance media, the cell sheet was washed twice with PBS, pH 7·4. Cultures were inoculated with 500 μl of virus dilution containing 200 p.f.u. Virus was allowed

Table 1. Viruses used in the study

SVDV isolate*	Material sequenced	GenBank accession no.	Reference
HKN '70†	–	AY429470	G. Ye and others, unpublished results
UKG 27/72	–	X54521	Seechurn *et al.* (1990)
J/1 '73†	–	D16364	Inoue *et al.* (1993)
H/3 '76†	–	D00435	Inoue *et al.* (1989)
NET 1/92	–	AF268065	Rebel *et al.* (2000)
AUR 1/73	Epithelium	AY875984	This study
SWI 1/74	Epithelium	AY875985	This study
FRA 1/73	Epithelium	AY875986	This study
HKN 1/82	Epithelium	AY875987	This study
HKN 1/89	IB-RS-2‡	AY875988	This study
HKN 3/89	IB-RS-2	AY875989	This study
HKN 18/87	IB-RS-2	AY875990	This study
ITL 2/92	IB-RS-2	AY875991	This study
ITL 1/66	IB-RS-2	AY875992	This study
HKN 19/70	Epithelium	AY875993	This study
HKN 3/81	Epithelium	AY875994	This study
ITL 19/92	Original field material	AY875995	This study
ITL 20/92	Original field material	AY875996	This study
ITL 8/94	Porcine kidney culture	AY875997	This study
ITL 1/92	Original field material	AY875998	This study
NET 3/92	IB-RS-2	AY875999	This study
HKN 1/80	Epithelium	AY876000	This study
ITL 1/97	IB-RS-2 and epithelium	AY876001	This study
ITL 2/97	IB-RS-2	AY876002	This study
ITL 3/97	IB-RS-2	AY876003	This study
ITL 13/99	IB-RS-2	AY876004	This study
POR 1/2003	Epithelium	AY876005	This study
SPA 1/93	IB-RS-2	AY876006	This study
ITL 10/2003	IB-RS-2	AY876007	This study
TAW 119/97	IB-RS-2	AY876008	This study
TAW 1/98	IB-RS-2	AY876009	This study
POR 3/95	IB-RS-2	AY876010	This study
BUL 2/71	Epithelium	AY876011	This study

*Food and Agriculture Organization of the United Nations/Office International des Epizooties (FAO/OIE) reference laboratory number.
†Not a FAO/OIE laboratory reference number.
‡Supernatant from IB-RS-2 cell line.

Table 2. Primer sequences used in this study

Primer name	Genome location*	Sequence (5′–3′)	PCR	Sequencing
SVD-5UTR FOR3	12–31	TGT GGG TTG TTC CCA CCC AC	√	
SVD-5UTR REV3	774–755	CCG GTC TTT TGT GTT GAC AC	√	
SVD-5UTR FOR1	64–85	CGG TAC CTT TGT GCG CCT GTT T		√
SVD-5UTR REV1	765–743	TGT GTT GAC AC(CT) TGA GCT CCC AT		√
SASVD-2B-IR-252-275F	252–275	CGA GAA ACC TAG TAC CAC CAT GAA		√
SASVD-2B-IR-332-312R	332–312	CGG TGA CTC ATC GAC CTG ATC		√
SASVD-3-IR-455-473F	455–473	CCC TGA ATG CGG CTA ATC C	√	√
SASVD-3-IR-522-503R	522–503	CCA TTA CGA CAG ACT GCC CA		√

*Genome locations according to GenBank accession no. X54521.

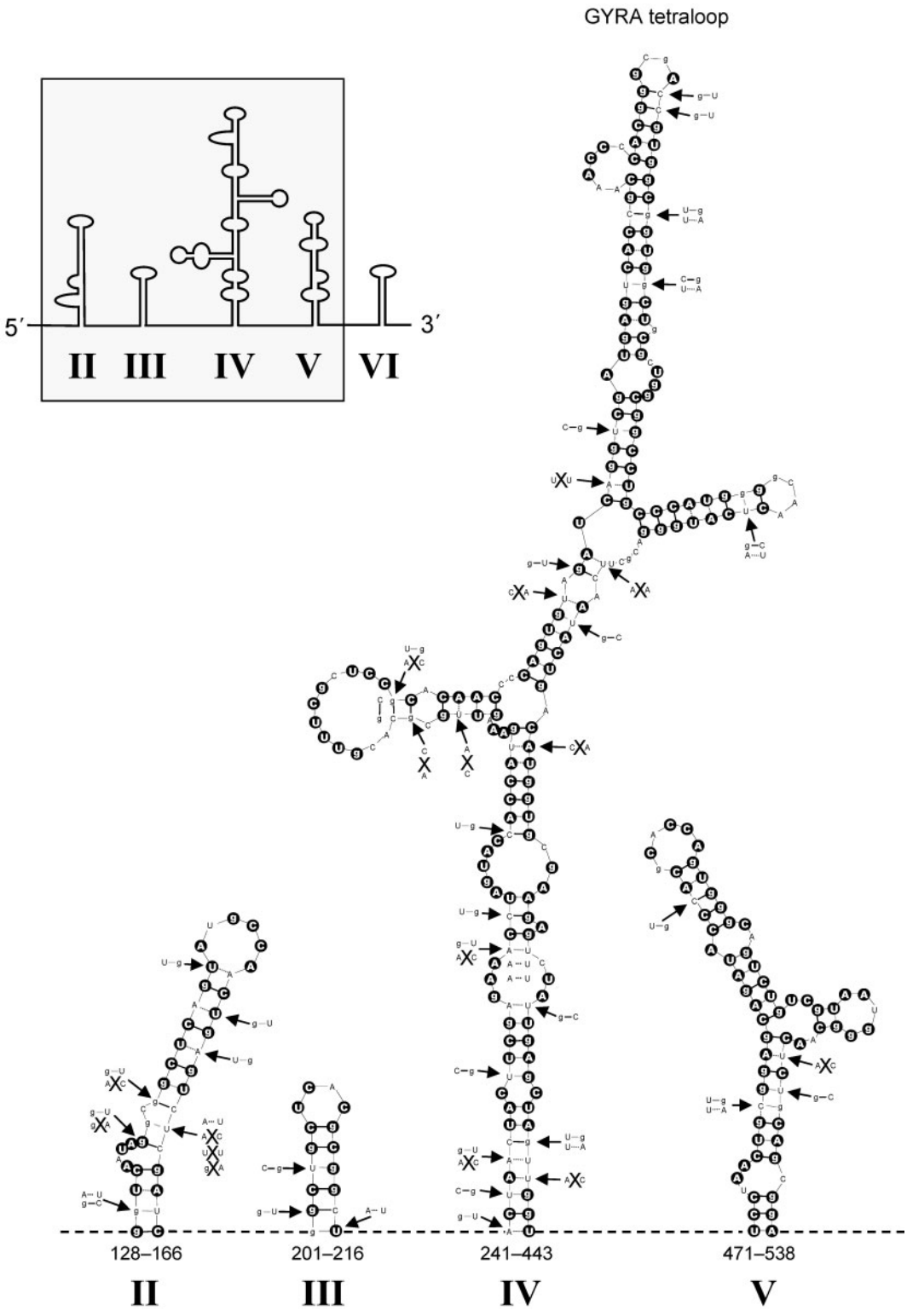

Fig. 1. Predicted RNA structure for four stem–loops (II to V) of the SVDV IRES. Sequence and numbering shown is for the reference isolate UKG 27/72 (accession no. X54521) with nucleotides with black circle background denoting positions conserved across all 33 SVDV isolates. Arrows denote compensatory substitutions resulting in alternative RNA base-pairing (g-C, A-U and g-U) or positions where the base-pairing does not result (nXn) among some of the remaining 32 SVDV isolates.

to adsorb for 30 min at 37 °C before adding 5 ml serum-free modified Eagles maintenance medium. Flasks of each virus were incubated at 37 °C or 32 °C (four replicates at each temperature). A sample from each flask was collected at 0, 12, 24, 48 and 72 h post-inoculation; 0·2 ml of the cell-culture supernatant fluid was removed, added to 1 ml Trizol reagent (Invitrogen) and stored at −80 °C until tested by real-time RT-PCR.

Real-time RT-PCR. RNA was extracted using the QIAamp extraction kit on a QIAamp BioRobot 9604 (Qiagen). A QIAamp BioRobot 3000 was then used for the liquid-handling steps of the reverse transcription and PCR procedures with pipetting volumes similar to those described before (Reid *et al.*, 2004b) and the 2B-IR primers/probe set (Reid *et al.*, 2004a). A dilution series of an RNA standard transcribed *in vitro* (MEGAscript, Ambion) from a plasmid clone containing the SVDV IRES (pGEM3Z/J1 IRES; Sakoda *et al.*, 2001) enabled viral genome (RNA copies in each sample) to be quantified, as described elsewhere (Inoue *et al.*, 2005). Each RNA standard dilution (6·0 µl) was added manually to reverse transcription reaction mix (9·0 µl) immediately before the reverse transcription incubation reaction, as previously described (Reid *et al.*, 2004b).

RESULTS

Nucleotide sequence analysis

Sequences were obtained from 28 SVDV isolates (GenBank accession nos AY875984–AY876011, Table 1). With the exception of isolate BUL 2/71, where sequencing difficulties were encountered at the 3′ end, the sequences were trimmed to a fragment corresponding to nucleotides 66–745 of the reference isolate UKG 27/72 (GenBank accession no. X54521), ending with the AUG start codon of the SVDV polyprotein. In addition to X54521, four other sequences available on GenBank were included in the data analysis. Some isolates (HKN 1/89 and HKN 3/89, ITL 1/97 and ITL 3/97) had identical sequences. In contrast, the lowest nucleotide identity between any two sequences calculated using BESTFIT (GCG) was 85·7 % for HKN 18/87 and TAW 1/98.

In common with the 5′ UTRs of other picornaviruses, a polypyrimidine tract approximately 20 nt upstream of a conserved cryptic AUG was present in all 33 SVDV sequences. Both these features have been shown to play a role in translation initiation (Pelletier *et al.*, 1988; Pilipenko *et al.*, 1995). As previously reported (Seechurn *et al.*, 1990), SVDV secondary-structure predictions reveal a picornaviral IRES structure similar to that proposed for poliovirus 3 (Skinner *et al.*, 1989; Le & Maizel, 1998). Fig. 1 shows the nucleotide base-pairing for four of these proposed stem–loop structures (designated stem–loops II to V; Beales *et al.*, 2003). It was difficult to reliably model the final stem–loop (VI) containing the cryptic AUG proposed for other enteroviruses (Semler, 2004) for all SVDV sequences, and it is therefore not shown in Fig. 1. A GNRA (GYRA) tetraloop (Jucker *et al.*, 1996) present in other picornavirus IRES elements (Semler, 2004) is generated (positions 345–348) at the apex of stem–loop IV. Interestingly, there was evidence for compensatory nucleotide substitutions at 25 positions in these four stem–loops in order to maintain RNA base-pairing (Fig. 1). These compensatory substitutions were located particularly at the apex and base of the stem–loops. In contrast, there was a degree of plasticity in the predicted structures generated in the middle of stem–loops II, IV and V.

The nucleotide sequence of the 5′ UTR spacer region of SVDV is highly variable

A high proportion (403/529, 76·2 %) of nucleotide positions in the 5′ UTR containing the IRES region (positions 66–589) were totally conserved across all 33 SVDV isolates. In contrast, even when gaps were excluded from the analysis, only 38/150 (25·3 %) of nucleotide positions were conserved in the spacer region located between the cryptic AUG (at position 590) and the start codon of the polyprotein (Fig. 2). Of particular interest was the finding of block deletions in eight SVDV isolates of between 6 and 125 nt in the spacer (Fig. 3). The largest deletion was found in the sequence for

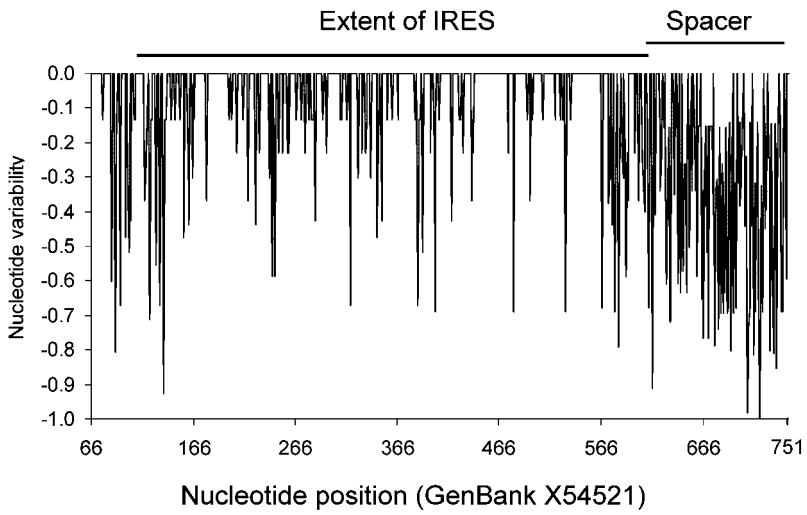

Fig. 2. Variability analysis (Proutski & Holmes, 1998) for the 5′ UTR of 33 SVDV isolates. Positions with gaps in the alignment were excluded from this analysis.

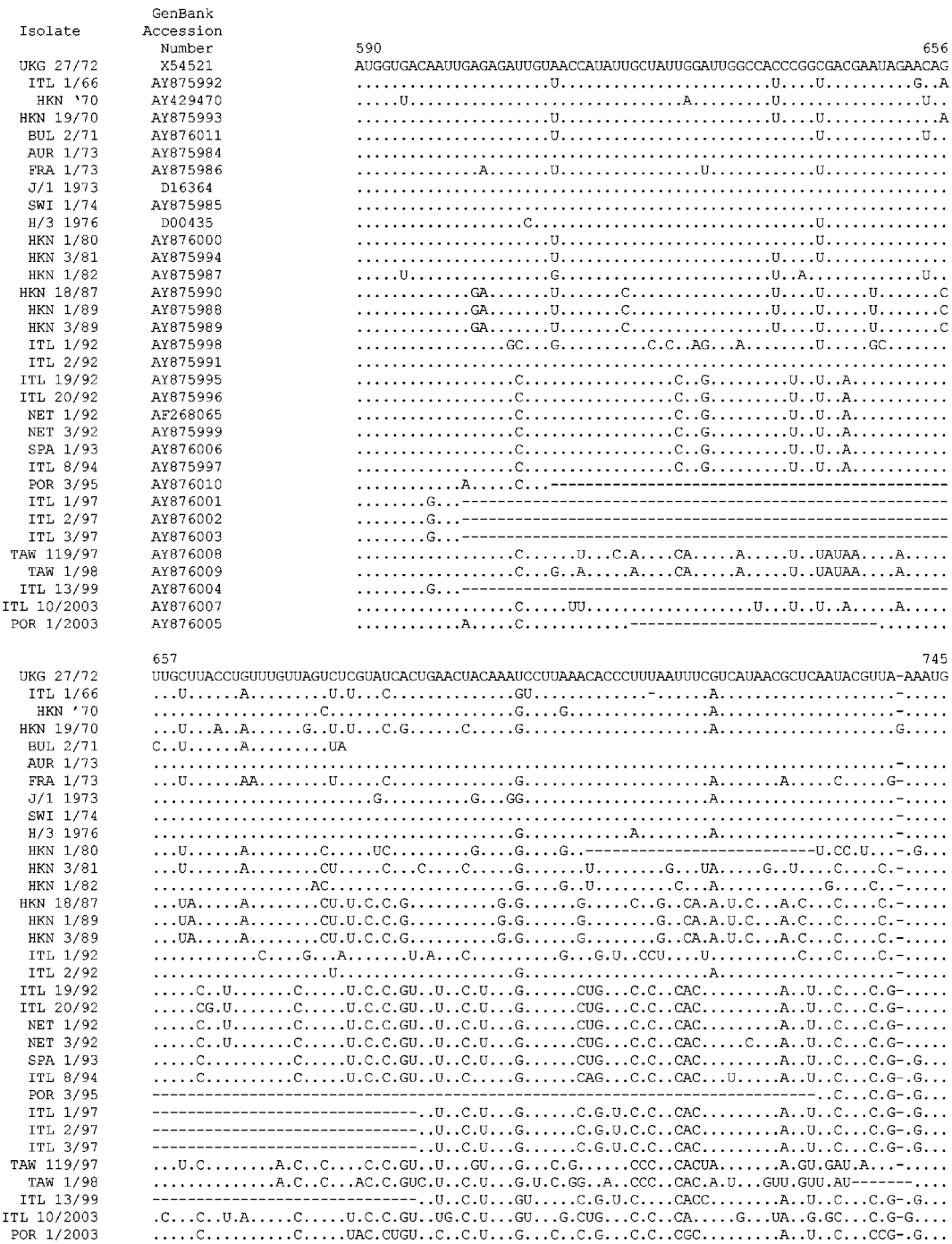

Fig. 3. Multiple sequence alignment for the 5′ UTR spacer region of 33 SVDV isolates. The alignment shown starts at the cryptic AUG and ends at the polyprotein initiation codon. Sequences with identity to the SVDV reference isolate UKG 27/72 (accession no. X54521) are represented as (.). Gaps (-) were inserted to maximize alignment. Numbering is based on the UKG 27/72 sequence.

the POR 3/95 isolate, resulting in a 5′ UTR almost devoid of the entire spacer region. Amplification of these regions using alternative PCR strategies, including primers targeting the deleted region, gave results consistent with the presence of deletions in these isolates (data not shown), indicating that these findings were not an artefact of PCR amplification. Furthermore, two of the sequences (from isolates HKN 1/80 and POR 1/2003) were obtained directly from clinical material. Identical sequences to those initially determined for the tissue culture ITL 1/97 isolate (Table 1) were also generated using RNA extracted from the original clinical material for this isolate. Together, these findings suggest that

the deletions were probably not an adaptation to growth in tissue culture. Phylogenetic analysis of the VP1 region showed that six of the eight isolates with these block deletions were closely related, belonging to a single lineage of Italian and Portuguese viruses (data not shown). Subsequent RT-PCR analysis revealed three additional SVDV isolates (POR 25/95, ITL 2/99 and ITL 5/98) with 5′ UTRs of similar size to those of members of this group (data not shown).

Reduced plaque size of SVDV isolates with 5′ UTR deletions

The mean plaque diameters (±SD) in IB-RS-2 cells of two SVDV isolates without spacer deletions (UKG 27/72 and SPA 1/93) were calculated to be 5·4±1·8 mm (n=93 determinations) and 5·2±1·0 mm (n=109), respectively. In contrast, significantly reduced plaque diameters (Fig. 4) were obtained for four viruses with spacer deletions [HKN 1/80, 4·2±1·7 mm (n=70); POR 1/2003, 3·8±1·4 mm (n=102); ITL 3/97, 3·1±1·5 mm (n=55); POR 3/95, 1·8±0·8 mm (n=104)]. A one-way analysis of variance was performed using MINITAB and revealed significant differences in plaque diameter between the viruses (F=94·98, P<0·001, MS=177·91). Post-hoc comparisons using Fisher's LSD test revealed significant differences in plaque diameter between all but two of the isolates. There was no significant difference between the mean plaque diameter of UKG 27/72 and SPA 1/93 (both viruses without deletions), and no significant difference between the mean plaque diameter of HKN 1/80 and POR 1/2003 (where there is only a single base difference in the deletion size). All viruses with a deletion in the 5′ UTR produced significantly smaller mean plaque diameters than both UKG 27/72 and SPA 1/93. The mean plaque diameter for POR 3/95 was significantly smaller than that of any of the other five isolates.

In vitro growth analysis

In vitro time-course experiments were performed to compare the growth of the SVDV isolates. Maximum viral copies in the supernatant as detected by real-time RT-PCR were

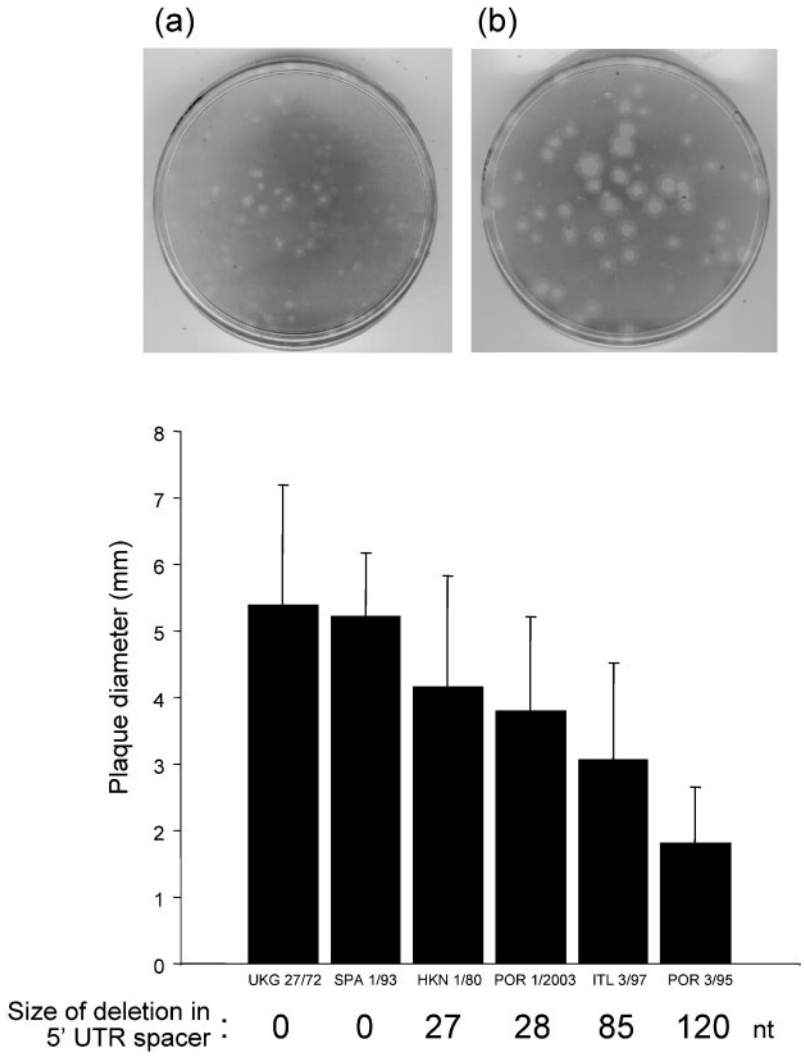

Fig. 4. Reduced plaque size in IB-RS-2 cell cultures of SVDV isolates with block deletions in the 5′ UTR spacer. Bars represent mean±SD for six SVDV isolates. Representative results (top) are shown for POR 3/95 (a) compared with SVDV reference strain UKG 27/72 (b).

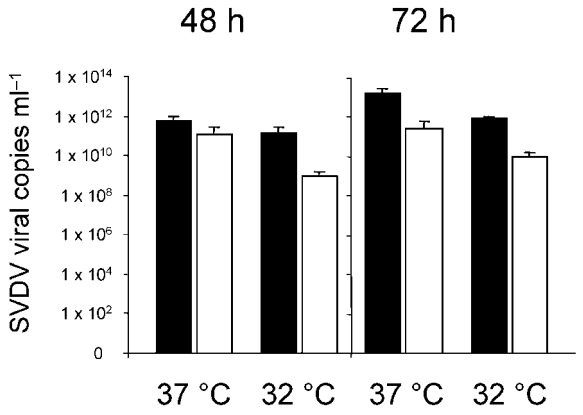

Fig. 5. Comparison between the SVDV genome copies detected by real-time RT-PCR in supernatant obtained from IB-RS-2 cells cultured for 24 and 48 h. Black bars and white bars represent results for UKG 27/72 and POR 3/95, respectively (mean value ± SD; $n = 4$ independent experiments).

generated after 48–72 h culture. POR 3/95 grew to a significantly ($P < 0{\cdot}05$) lower final titre relative to UKG 27/72 (Fig. 5) after 72 h incubation at 37 °C. This difference was also evident after incubation of the cultures at 32 °C, although the final viral titre for both of the viruses was reduced.

DISCUSSION

This paper presents 5′ UTR sequences for 28 representative SVDV isolates. The region sequenced includes the IRES, which plays a critical role in cap-independent translation of the viral polyprotein. Based on detailed studies of other picornaviruses, SVDV and other enteroviruses share an IRES morphology in common with rhinoviruses, and are collectively classified as having type I IRESs (Jackson *et al.*, 1990; Beales *et al.*, 2003). In addition to the high number of conserved nucleotides in the IRES, there was evidence for compensatory substitutions to maintain RNA base-pairing in the stems of the loop structures. Other critical features of the 5′ UTR, such as the oligopyrimidine/AUG tandem (OAT) were also present in all sequences. Together, these data support the use of segments within this region for sensitive diagnostic RT-PCR assays for the detection of SVDV. Of the two existing real-time RT-PCR assays (2B-IR; Reid *et al.*, 2004a), one is located entirely in stem–loop IV, with 19/24 nt of the 2B-IR forward primer; 17/21 nt of the 2B-IR reverse primer and 19/21 nt of the 2B-IR probe conserved across all of the SVDV isolates sequenced. The second assay (3-IR; Reid *et al.*, 2004a) is situated partially in stem–loop V, stretching into the neighbouring 5′ flanking region (from position 455). Although the forward primer used for this assay is totally conserved (at 19/19 nucleotide positions), critical changes at two positions in the probe region are responsible for its failure to detect a number of SVDV isolates [including ITL 19/92 (Reid *et al.*, 2004a) and more-recent (2003–2004) isolates from Italy (data not shown)]. The sequence alignment reveals blocks of invariant nucleotides (358–383, 442–474 and 537–566) which may be suitable for the design of improved real-time RT-PCR assays for the detection of SVDV.

In contrast to the relative conservation of the IRES element, there was considerable nucleotide variability in the spacer region located after the cryptic AUG. Interestingly, this study also highlighted the presence of block deletions of between 6 and 125 nt in this region for a number of SVDV isolates. A close ancestral relationship was shared among nine of the 11 isolates shown to have a deletion. It is possible to speculate that the largest deletion (POR 3/95) is a product of stepwise (28–85–125) deletions observed in other SVDV isolates. Some of these sequences with deleted regions (HKN 1/80 and POR 1/2003) were recovered directly from clinical material from infected animals, suggesting that these unexpected findings did not necessarily arise through tissue-culture adaptation.

In vitro growth studies showed that selected isolates with these deletions had a significantly reduced plaque diameter, a finding similar to observations with artificially generated mutants of poliovirus 1 (Gmyl *et al.*, 1993; Slobodskaya *et al.*, 1996). Furthermore, POR 3/95 grows to a significantly lower titre than the reference strain UKG 27/72. It is attractive to speculate that these effects relating to the *in vitro* viral growth of these selected SVDV isolates are related to the remarkable deletions evident in their 5′ UTR. However, since the region sequenced in this study only contributes a minor proportion of the total SVDV genome length, it is impossible to rule out the influence of changes elsewhere in these viruses. The mechanism of this effect on viral growth is not clear. One possible explanation is that these effects could be related to the ability of these viruses to form the final stem–loop VI of the IRES (Beales *et al.*, 2003) containing the cryptic AUG, or may simply be the result of a shorter distance between critical motifs in this region. There was a striking similarity between the length of the spacer for POR 3/95 and that of rhinovirus 14 (Callahan *et al.*, 1985). However, there was no evidence for a differential effect of temperature, as might be expected for a respiratory phenotype.

In summary, this paper describes sequences for the 5′ UTR of SVDV which unexpectedly reveal the presence of block deletions in the genome of some isolates. Of further interest is the finding that viruses with these deletions grow less well in cell culture. It is possible that these *in vitro* observations may reflect altered *in vivo* characteristics for these viruses. Indeed, previous studies have shown that plaque size can be correlated to the pathogenicity of SVDV, although in an earlier study these effects were mapped to the 2A region of the genome (Kanno *et al.*, 1999). Further work is required to define the significance of the deletions highlighted by this study and to assess whether they impact upon SVD.

ACKNOWLEDGEMENTS

This work was funded by the Department for Environment, Food and Rural Affairs (DEFRA) (projects SE1119 and SE1120). The authors would like to thank Graham Belsham for his helpful discussions and donation of the plasmid pGEM3Z/J1 IRES.

REFERENCES

Beales, L. P., Holzenburg, A. & Rowland, D. J. (2003). Viral internal ribosome entry site structures segregate into two distinct morphologies. *J Virol* **77**, 6574–6579.

Belak, S. & Thoren, P. (2001). Molecular diagnosis of animal diseases: some experiences over the past decade. *Expert Rev Mol Diagn* **1**, 434–443.

Belsham, G. J. & Jackson, R. J. (2000). Translational control of gene expression. In *Translation Initiation on Picornavirus RNA*, pp. 869–900. Edited by N. Sonenberg, J. W. B. Hershey & M. B. Matthews. Cold Spring Harbor, NY: Cold Spring Harbor Laboratory.

Brocchi, E., Zhang, G., Knowles, N. J., Wilsden, G., McCauley, J. W., Marquardt, O., Ohlinger, V. F. & De Simone, F. (1997). Molecular epidemiology of recent outbreaks of swine vesicular disease: two genetically and antigenically distant variants in Europe, 1987–1994. *Epidemiol Infect* **118**, 51–61.

Callahan, P. L., Mizutani, S. & Colonno, R. J. (1985). Molecular cloning and complete sequence determination of RNA genome of human rhinovirus 14. *Proc Natl Acad Sci U S A* **82**, 732–736.

De Castro, M. P. (1964). Behaviour of the foot and mouth disease virus in cell cultures: susceptibility of the IB-RS-2 line. *Arch Inst Biol (Sao Paulo)* **31**, 63–78.

Dekker, A., Moonen, P., deBoer-Luijtze, E. A. & Terpstra, C. (1995). Pathogenesis of swine vesicular disease after exposure of pigs to an infected environment. *Vet Microbiol* **45**, 243–250.

Fallacara, F., Pacciarini, M. L., Bugnetti, M., Berlinzani, A. & Brocchi, E. (2000). Detection of swine vesicular disease virus in faeces samples by immune-PCR assay. In *Proceedings of the 5th International Congress of the European Society for Veterinary Virology, Brescia, Italy, 27–30 August 2000*, pp. 173–174. Edited by E. Brocchi and A. Lavazza.

Ferris, N. P. & Dawson, M. (1988). Routine application of enzyme-linked immunosorbent assay in comparison with complement fixation for the diagnosis of foot-and-mouth and swine vesicular diseases. *Vet Microbiol* **6**, 201–209.

Garland, A. J. M. & Mann, J. A. (1974). Attempts to infect pigs with coxsackie virus type B5. *J Hyg* **73**, 85–96.

Gmyl, A. P., Pilipenko, E. V., Maslova, S. V., Beloy, G. A. & Agol, V. I. (1993). Functional and genetic plasticities of the poliovirus genome: quasi-infectious RNAs modified in the 5′-untranslated region yield a variety of pseudorevertants. *J Virol* **67**, 6309–6316.

Inoue, T., Suzuki, T. & Sekiguchi, K. (1989). The complete nucleotide sequence of swine vesicular disease virus. *J Gen Virol* **70**, 919–934.

Inoue, T., Yamaguchi, S., Kanno, T., Sugita, S. & Saeki, T. (1993). The complete nucleotide sequence of a pathogenic swine vesicular disease virus isolated in Japan (J1′73) and phylogenetic analysis. *Nucleic Acids Res* **21**, 3896.

Inoue, T., Alexandersen, S., Clark, A. T., Murphy, C., Quan, M., Reid, S. M., Sakoda, Y., Johns, H. L. & Belsham, G. J. (2005). Importance of arginine 20 of the swine vesicular disease virus 2A protease for activity and virulence. *J Virol* **79**, 428–440.

Jackson, R. J., Howell, M. T. & Kaminski, A. (1990). The novel mechanism of initiation of picornavirus RNA translation. *Trends Biochem Sci* **15**, 477–483.

Jucker, F. M., Heus, H. A., Yip, P. F., Moors, E. H. & Pardi, A. (1996). A network of heterogenous hydrogen bonds in GNRA tetraloops. *J Mol Biol* **264**, 968–980.

Kanno, T., Mackay, D., Inoue, T. & 7 other authors (1999). Mapping the genetic determinants of pathogenicity and plaque phenotype in swine vesicular disease virus. *J Virol* **73**, 2710–2716.

Le, S. Y. & Maizel, J. V. (1998). Evolution of a common structural core in the internal ribosome entry sites of picornavirus. *Virus Genes* **16**, 25–38.

Mathews, D. H., Sabina, J., Zuker, M. & Turner, D. H. (1999). Expanded sequence dependence of thermodynamic parameters improves prediction of RNA secondary structure. *J Mol Biol* **288**, 911–940.

Nardelli, L., Lodetti, G., Gualandi, G. L., Burrows, R., Goodridge, D., Brown, F. & Cartwright, B. (1968). A foot-and-mouth disease syndrome in pigs caused by an enterovirus. *Nature* **219**, 1275–1276.

Pelletier, J., Flynn, M. E., Kaplan, G., Racaniello, V. & Sonenberg, N. (1988). Mutational analysis of upstream AUG codons in poliovirus RNA. *J Virol* **62**, 4486–4492.

Pilipenko, E. V., Gmyl, A. P. & Agol, V. I. (1995). A model for rearrangements in RNA genomes. *Nucleic Acids Res* **23**, 1870–1875.

Proutski, V. & Holmes, E. (1998). SWAN: sliding window analysis of nucleotide sequence variability. *Bioinformatics* **14**, 467–468.

Rebel, J. M., Leendertse, C. H., Dekker, A., van Poelwijk, F. & Moormann, R. J. (2000). Construction of a full-length infectious cDNA clone of swine vesicular disease virus strain NET/1/92 and analysis of new antigenic variants derived from it. *J Gen Virol* **81**, 2763–2769.

Reid, S. M., Ferris, N. P., Hutchings, G. H., King, D. P. & Alexandersen, S. (2004a). Evaluation of real-time reverse transcription polymerase chain reaction assays for the detection of swine vesicular disease virus. *J Virol Methods* **116**, 169–176.

Reid, S. M., Paton, D. J., Wilsden, G., Hutchings, G. H., King, D. P., Ferris, N. P. & Alexandersen, S. (2004b). Use of automated real-time RT-PCR to monitor experimental swine vesicular disease virus infection in pigs. *J Comp Pathol* **131**, 308–317.

Sakoda, Y., Ross-Smith, N., Inoue, T. & Belsham, G. J. (2001). An attenuating mutation in the 2A protease of swine vesicular disease virus, a picornavirus, regulates cap- and internal ribosome entry site-dependent protein synthesis. *J Virol* **75**, 10643–10650.

Seechurn, P., Knowles, N. J. & McCauley, J. W. (1990). The complete nucleotide sequence of a pathogenic swine vesicular disease virus. *Virus Res* **16**, 255–274.

Semler, B. L. (2004). Poliovirus proves IRES-istible in vivo. *J Clin Invest* **113**, 1678–1681.

Skinner, M. A., Racaniello, V. R., Dunn, G., Cooper, J., Minor, P. D. & Almond, J. W. (1989). New model for the secondary structure of the 5′ non-coding RNA of poliovirus is supported by biochemical and genetic data that also show that RNA secondary structure is important in neurovirulence. *J Mol Biol* **207**, 379–392.

Slobodskaya, O. R., Gmyl, A. P., Maslova, S. V., Tolskaya, E. A., Viktorova, E. G. & Agol, V. I. (1996). Poliovirus neurovirulence correlates with the presence of a cryptic AUG upstream of the initiator. *Virology* **221**, 141–150.

Thompson, J. D., Higgins, D. G. & Gibson, T. J. (1994). CLUSTAL W: improving the sensitivity of progressive multiple sequence alignment through sequence weighting, position-specific gap penalties and weight matrix choice. *Nucleic Acids Res* **22**, 4673–4680.

Zhang, G., Haydon, D. T., Knowles, N. J. & McCauley, J. W. (1999). Molecular evolution of swine vesicular disease virus. *J Gen Virol* **80**, 639–651.